Monthly Notices
of the
ROYAL ASTRONOMICAL SOCIETY

Mon. Not. R. Astron. Soc. **408,** 2476–2486 (2010) doi:10.1111/j.1365-2966.2010.17304.x

Asymptotic giant branch stars at low metallicity: the challenging interplay between the mass-loss and molecular opacities

P. Ventura[1]⋆ and P. Marigo[2]

[1]*INAF-Osservatorio Astronomico di Roma, Via Frascati 33, 00040 Monte Porzio Catone, Italy*
[2]*Department of Astronomy, University of Padova, Vicolo dell'Osservatorio 3, I-35122 Padova, Italy*

Accepted 2010 July 2. Received 2010 July 2; in original form 2010 February 13

ABSTRACT

We investigate the main physical properties of low-metallicity asymptotic giant branch (AGB) stars with the aim of quantifying the uncertainties that presently affect the predicted chemical yields of these stars, associated with the mass-loss and description of molecular opacities. We find that above a threshold mass, $M \simeq 3.5\,\mathrm{M}_{\odot}$ for $Z = 0.001$, the results are little dependent on the opacity treatment, as long as the hot-bottom burning (HBB) prevents the surface C/O ratio from exceeding unity; the yields of these massive AGB stars are expected to be mostly determined by the efficiency of convection, with a relatively mild dependence on the mass-loss description. A much higher degree of uncertainty is associated with the yields of less-massive models, which critically depend on the adopted molecular opacities. An interval of masses exists, say, 2.0–3.0 $\mathrm{M}_{\odot}$ (the exact range depends on the mass-loss), in which the HBB may be even extinguished following the cooling produced by the opacity of C-bearing molecules. The yields of these stars are the most uncertain, the variation range being the largest (up to ∼2 dex) for the nitrogen and sodium yields. For very low mass models, not experiencing the HBB ($M \leq 1.5\,\mathrm{M}_{\odot}$), the description of mass-loss and the treatment of the convective boundaries are crucial for the occurrence of the third dredge-up, with a sizeable impact on the CNO yields.

Key words: stars: abundances – stars: AGB and post-AGB.

1 INTRODUCTION

The asymptotic giant branch (AGB) is a common phase of the evolution of stars with masses in the range 1–8 $\mathrm{M}_{\odot}$ (Busso, Gallino & Wasserburg 1999; Herwig 2005). After core-helium burning, they experience a series of thermal pulses (TPs) triggered by the ignition of helium in a thin layer below the CNO burning shell, under conditions of thermal instability. The strong mass-loss that they experience favours the ejection of the whole external mantle, with the formation of a CO white dwarf.

Historically, the interest towards AGBs grew up with the discovery of s-process-enriched AGB stars (Merrill 1952) and with their identification as sites of nucleosyntheses and s-processes (Burbidge et al. 1957), and was further stimulated by the discovery of carbon- and lithium-rich stars in the Galaxy and the Magellanic Clouds (MCs) (Blanco, Blanco & McCarthy 1980; Smith & Lambert 1989, 1990; Abia et al. 1991): they were correctly interpreted as thermally pulsating stars (Iben & Renzini 1982; Sackmann & Boothroyd 1992). Extended investigations of the physical properties of AGB stars showed the existence of two mechanisms capable of altering the surface chemistry: the third dredge-up (TDU), that is, the inward penetration (in mass) of the external envelope, after each TP, into regions earlier involved in 3α nucleosyntheses (Iben 1975; Fujimoto, Nomoto & Sugimoto 1976) and the hot-bottom burning (HBB), when the base of the convective envelope becomes sufficiently hot ($\geq 40 \times 10^6$ K), to produce p-capture nucleosyntheses (Scalo, Despain & Ulrich 1975; Renzini & Voli 1981) and enough energy to cause the breakdown of the core mass–luminosity relation on the AGB (Blöcker & Schöenberner 1991; Boothroyd & Sackmann 1992).

In more recent years, we have been gathering the compelling evidence that thermally pulsating AGB (TP-AGB) stars play a crucial role in many properties of their host systems, mainly owing to their intrinsic brightness and distinctive spectral features. For instance, the TP-AGB contribution to the total luminosity of single-burst stellar populations reaches a maximum of about 40 per cent at ages from 1 to 3 Gyr (Frogel, Mould & Blanco 1990) and accounts for most of the bright infrared objects in resolved galaxies, as clearly demonstrated by DENIS, 2MASS, SAGE, S^{3}MC and AKARI IRC data (Cioni et al. 1999; Nikolaev & Weinberg 2000; Blum et al. 2006; Bolatto et al. 2007; Ita et al. 2008) for the MCs. Now, observational data of AGB stars are also available for other galaxies of the Local Group, such as Leo I (Held et al. 2010), Leo II (Gullieuszik

⋆E-mail: ventura@oa-roma.inaf.it

et al. 2008), Sagittarius (Gullieuszik et al. 2007), Phoenix (Menzies et al. 2008) and Fornax (Whitelock et al. 2009), as well as for more distant dwarf galaxies.[1]

Chemical pollution from massive AGB stars is currently one of the most plausible hypotheses to account for the chemical patterns observed in globular cluster (GC) stars (Carretta 2006), where they may explain the existence of multiple populations (Ventura et al. 2001), indicated by the discovery of multiple main sequences in some GCs (Piotto et al. 2007). The pioneering model by D'Ercole et al. (2008) outlines the capability of massive AGB stars to provide an efficient pollution of the interstellar medium and to stimulate the formation of new stellar generations, with predicted photometric and spectroscopic properties consistent with observations.

Moving from the zero to high redshifts, the light contribution from AGB stars becomes significant in the optical, where galaxies are dominated by intermediate-age stars (Bressan, Chiosi & Fagotto 1994; Bruzual & Charlot 2003; Maraston 2005). This fact is crucial: it has been recently pointed out that quantifying the weight of TP-AGB stars has a large impact on the mass assembly in high-redshift galaxies (Santini et al. 2009).

The prominent role played by AGB stars in so many astrophysical contexts has increased the demand for detailed AGB modelling. Since full computations of the TP-AGB phase are extremely time-consuming, given the short time-steps that must be used during each TP, many synthetic models have been developed and are presently used, in which, based on the existing full models, the AGB properties are parametrized as a function of the stellar mass and metallicity (van den Hoek & Groenewegen 1997; Marigo, Girardi & Bressan 1999; Izzard et al. 2004; Marigo & Girardi 2007).

Unfortunately, the full AGB modelling is dependent on the assumptions on many physical ingredients that are not known from first principles and must be described by means of semi-empirical calibrations. The treatment of convection is regarded as the main reason for the large differences among AGB models in the existing literature: the efficiency of the convective instability and the assumptions concerning the extension of the mixed regions have a strong impact on the physical and chemical evolution of massive AGB stars (Herwig 2000, 2005; Ventura & D'Antona 2005).

Recent investigations have also shown that the main evolutionary properties of AGB stars can be critically affected by the radiative low-T opacities adopted to model their outer mantles. The use of opacities that correctly account for the drastic changes in the molecular chemistry of the gas, when the C/O ratio passes from below to above unity, is mandatory; otherwise, the general expansion of the outer layers triggered by the opacity increase is missed (Marigo 2002). Since one of the most significant consequences of a correct computation of the molecular opacities is a sudden increase in the mass-loss, a careful study of the effects driven by molecular opacities on the evolutionary properties and stellar yields requires to investigate the impact of the mass-loss and its uncertainties.

In order to produce more reliable full AGB models that may also contribute a useful input to synthetic AGB models, we have started a new project dedicated, in the first phase, to understand and quantify the main uncertainties associated with the various input physics.

The properties of the most massive AGB stars and the relevant role played by convection modelling were analysed by Ventura & D'Antona (2005). Moving to lower masses, Ventura & Marigo (2009) have discussed the role played by molecular opacities. In this work, we concentrate on how the opacity treatment is interfaced with the description of the mass-loss and which results in the literature need a substantial revision. Future steps will be an extensive comparison of model predictions with observations to provide the astrophysical community with more reliable yields.

This paper is organized as follows. Section 2 summarizes the uncertainties affecting AGB models. The physical ingredients of the models presented in the present investigation are detailed in Section 3. Section 4 is dedicated to the analysis of the physical properties of the models and how they depend on the choices concerning the opacity and mass-loss. The reliability of the yields and the expected chemical patterns are discussed in Section 5. A comparison with the results from other investigations on the same topic is presented in Section 6.

2 ABOUT THE UNCERTAINTIES AFFECTING ASYMPTOTIC GIANT BRANCH MODELLING

The theoretical description of the AGB evolution is extremely sensitive to the input physics used to calculate the models: the treatment of the convective instability, the description of the mass-loss, the extent of the possible extramixing region beyond the formal convective/radiative boundary determined by the classic Schwartzschild criterion, the adopted low-T opacities and the nuclear cross-sections of some p- and α-capture reactions. An exhaustive analysis can be found in Herwig (2005).

Ventura & D'Antona (2005), following the analysis by Blöcker & Schöenberner (1991) and Renzini & Voli (1981), showed that convection modelling plays an important role in determining the evolution during the TP phase: the differences in the convection modelling have been recognized as the main cause responsible for the discrepancies among the results obtained by different groups (Denissenkov & Herwig 2003; Fenner et al. 2004; Karakas & Lattanzio 2007).

The assumption of some convective overshoot[2] from the bottom of the envelope is closely associated with the occurrence of a TDU after a TP, which, in turn, is confirmed by the discovery of many carbon stars in the Galaxy and in the MCs (see e.g. Battinelli & Demers 2004; Groenewegen et al. 2009). The analyses by Groenewegen & de Jong (1993) and Marigo et al. (1999), based on synthetic TP-AGB models, indicate that the extent of the TDU required to reproduce the luminosity function of the MCs should be larger than predicted by the standard models, where a TDU is found in the context of the Schwarzschild criterion.

With respect to the mass-loss along the AGB, several prescriptions, based on either theoretical or empirical grounds, have been proposed in the literature. Among them we recall: Reimers' (1975) classical law was a fit of measured mass-loss rates as a function of MR/L; Vassiliadis & Wood (1993) (hereinafter VW93) was based on the observed correlation between mass-loss rates and periods of pulsating AGB stars; Blöcker (1995) proposed a modification to the Reimers' law based on fitting models from Bowen (1988); Bowen & Willson (1991) presented a prescription based on dynamical models of pulsating oxygen-rich atmospheres, including the formation of dust; based on those models Bedijn (1988) derived a mass-loss formalism as a function of basic stellar parameters M, R and $T_{\rm eff}$; Wachter et al. (2002, 2008) proposed a formula based on dust-driven superwind models of C stars; van Loon et al. (2005)

[1] HST prop. 11719.

[2] By convective overshoot, we mean the further distance travelled by convective eddies beyond the border, where buoyancy vanishes, fixed by the Schwarzschild criterion.

presented an empirical calibration based on observations of dust-enshrouded red supergiants and oxygen-rich AGB stars; Schröder & Cuntz (2005) introduced a correction to the Reimers' formula based on some physical arguments; and Straniero, Gallino & Cristallo (2006) (hereinafter S06) formulated a revised calibration of the mass-loss–period relation for pulsating AGB stars.

In AGB models, an additional source of uncertainty is related to the adopted low-T radiative opacities, which quantify the removal of radiation energy as photons pass through the H-rich mantle. The early predictions by Marigo (2002) were confirmed by Cristallo et al. (2008), who showed how the physical and chemical evolution of low-mass, low-Z stars is affected by the adoption of the correct opacity treatment.

3 PHYSICAL AND CHEMICAL INPUTS

The models presented in this paper were calculated by means of the ATON code for stellar evolution (Mazzitelli 1979), a full description of which can be found in Ventura et al. (1998).

3.1 Convective regions

Convection was modelled according to the Full Spectrum of Turbulence prescription by Canuto & Mazzitelli (1991). The mixing of chemicals and the nuclear burning were coupled by means of a diffusive approach, following the scheme presented in Cloutman & Eoll (1976); accordingly, a convective overshoot was modelled by an exponential decay of convective velocities beyond the formal borders, with an e-folding decay of $l = \zeta H_P$. During the two main phases of the core nuclear burning and in the occurrence of the second dredge-up, we used $\zeta = 0.02$, in agreement with the calibration based on the width of the main sequences of open clusters given in Ventura et al. (1998). During the TP-AGB phase, given the uncertainties outlined in the previous section, no overshoot was considered.

3.2 Mass-loss

To investigate the sensitivity of the results obtained on the mass-loss prescription, our choice was to compare the findings obtained with two different prescriptions, namely Blöcker (1995) and S06. In the former case, it is assumed that, based on hydrodynamical simulations (Bowen 1988), there is a steep increase in the mass-loss with the increasing luminosity as the star enters the AGB phase. This is simulated by multiplying the canonical Reimers' formula by a luminosity power ($L^{2.7}$). The free parameter entering the Reimer's prescription is $\eta_{\rm R} = 0.02$, according to the calibration of the luminosity function of lithium-rich stars observed in the MCs given in Ventura, D'Antona & Mazzitelli (2000).

In S06, the mass-loss rate is made to vary with the pulsation period in the fundamental mode: compared to VW93, the empirical revision by S06 (see their fig. 5), based on a compilation of more recent data, predicts larger mass-loss rates for pulsation periods in the range 100–300 d, whilst lower rates are associated with periods larger than 500 d.

3.3 Equation of state and opacities

For the equation of state (EOS), we have adopted the latest version of the OPAL EOS (2005) where available, superseded by the Saumon, Chabrier & Van Horn (1995) EOS in the partial ionization regime. The EOS is extended to the high-density, high-temperature regime according to the description given in Stoltzmann & Blöcker (2000).

The radiative opacities were calculated following the OPAL prescription, according to Iglesias & Rogers (1996). The conductive opacities were taken from Poteckin (2006; see the web page http://www.ioffe.rssi.ru/astro/conduct/).

As to the low-T opacities, that is, $1500 \leq T \leq 10\,000$ K, we have used the same large data set of tables as used in Ventura & Marigo (2009), which were computed with the ÆSOPUS tool (Marigo & Aringer 2009)[3] to consistently follow the significant changes in the CNO surface abundances caused by the TDU and HBB during the TP-AGB evolution.

The opacity set was designed to account for the complex interplay between the convection and nucleosynthesis, so that variations in the C/O ratio can be driven by positive/negative changes in both carbon and oxygen abundances. For instance, while an increment of C/O is predicted due to the TDU, when the HBB takes place, the C/O ratio is expected either to decrease, as long as C is converted into N by the CN cycle, or to increase, if O is efficiently burnt in favour of N by the ON cycle (see Section 4.3).

Variations in CNO abundances affect the low-T opacities essentially in two ways: (i) for $T \lesssim 3000$ K, by modifying the equilibrium molecular pattern, depending on the C/O ratio; and (ii) to a less extent, for larger temperatures, by changing the contributions of the CNO atoms to both the continuum and line opacity. A detailed discussion can be found in Marigo & Aringer (2009; see their section 4.2) and Ventura & Marigo (2009).

3.4 Nuclear reactions

The nuclear network included in the code is described in details in Ventura & D'Antona (2005). The cross-sections of the 64 reactions considered are taken from the NACRE compilation (Angulo et al. 1999), with the exception of ^{14}N(p,γ)^{15}O taken from Formicola et al. (2004) and the three p-capture reactions of the Ne–Na cycle taken from Hale et al. (2002), for the ^{22}Ne(p,γ)^{23}Na reaction and from Hale et al. (2004) for the two p-captures by sodium nuclei.

4 EVOLUTIONARY PROPERTIES

4.1 An overview of the models

The stellar models discussed here were followed from the pre-main-sequence phase to almost the complete ejection of the external envelope. The initial chemical composition of the gas is assigned a total metallicity (mass fraction) $Z = 0.001$ and a degree of α-enhancement $[\alpha/{\rm Fe}] = +0.4$, with the reference solar mixture taken from Grevesse & Sauval (1998).

To investigate how much the results are affected by the the interplay between the use of the opacities accounting for the CNO variations and the mass-loss description, we calculated four sets of evolutionary models designated with S06H, S06C, BH and BC, which differ in the adopted prescriptions as outlined in Table 1. Specifically, we consider two formalisms for the mass-loss, that is, S06 and Blöcker (1995), and two treatments of the low-T opacities, depending on whether the underlying chemical mixture is kept fixed or accounts for changes in the CNO abundances. In order to better disentangle the effects of each prescription, the models cover all four combinations of the two parameters, opacity and mass-loss.

[3] ÆSOPUS web interface at http://stev.oapd.inaf.it/aesopus

Table 1. Input prescriptions of the TP-AGB models.

Model	Low-T opacities: CNO variations	Mass-loss	Symbol/line[a]
S06H	No	S06	▲/dashed
S06C	Yes	S06	○/long-dashed
BH	No	Blöcker (1995)	△/solid
BC	Yes	Blöcker (1995)	■/dotted

[a]Symbols and line styles used in the plots.

The resulting physical and chemical properties of the TP-AGB models described above are presented in Table 2. For each stellar mass, we show the number of TPs (NTP) experienced by the star, the final core mass, the maximum temperature reached at the bottom of the external envelope, plus further information concerning the average content of the ejecta, namely the helium mass fraction and the C, N, O and Na enhancement/depletion factors, in terms of the quantities [X/Fe], where $[X/\mathrm{Fe}] = \log(X/\mathrm{Fe}) - \log(X/\mathrm{Fe})_{\odot}$. The last column shows the ratio between the average C+N+O abundance in the ejecta and the initial value, which is assumed to represent the chemical mixture at the epoch of the star's formation.

4.2 The interplay between the mass-loss and molecular opacities

We can appreciate the qualitative effects of the different descriptions of the mass-loss and molecular opacities from Fig. 1, where we show the evolution of a 3-$M_{\odot}$ model calculated according to the prescriptions listed in Table 1, which we refer for the meaning of

Table 2. Relevant properties of AGB models.

$M/M_{\odot}$	NTP	$M_C/M_{\odot}$	$\log(T_{bce}^{max})$	Y	[^{12}C/Fe]	[^{14}N/Fe]	[^{16}O/Fe]	[Na/Fe]	R(CNO)
BH models									
6.00	24	1.029	8.05	0.347	−0.707	1.325	−0.369	0.248	0.929
5.50	28	0.987	8.05	0.340	−0.686	1.350	−0.468	0.283	0.946
5.00	33	0.947	8.02	0.329	−0.505	1.458	−0.410	0.402	1.205
4.50	34	0.916	8.00	0.312	−0.233	1.669	−0.112	0.674	2.012
4.00	33	0.888	7.97	0.293	0.090	1.781	0.191	0.935	2.850
3.50	28	0.857	7.94	0.270	0.259	1.902	0.464	1.147	4.074
3.00	24	0.822	7.88	0.250	0.796	1.942	0.678	1.123	5.518
2.50	22	0.746	7.49	0.257	1.805	0.519	0.985	0.416	11.204
2.00	20	0.702	7.05	0.261	1.564	0.463	0.622	0.346	6.015
BC models									
6.00	25	1.028	8.05	0.348	−0.706	1.323	−0.360	0.252	0.929
5.50	30	0.983	8.04	0.335	−0.667	1.362	−0.470	0.285	0.971
5.00	33	0.946	8.02	0.329	−0.527	1.479	−0.390	0.418	1.258
4.50	35	0.916	8.00	0.311	−0.175	1.609	−0.133	0.614	1.795
4.00	32	0.886	7.97	0.292	0.121	1.758	0.190	0.912	2.747
3.50	27	0.856	7.94	0.266	0.360	1.872	0.494	1.104	4.012
3.00	22	0.821	7.63	0.250	1.226	1.336	0.687	0.397	4.477
2.50	18	0.742	7.25	0.257	1.684	0.516	0.988	0.396	9.322
2.00	16	0.677	6.88	0.265	1.710	0.481	0.897	0.354	9.065
1.50	12	0.648	7.40	0.251	0.310	0.044	0.400	0.030	1.129
S06H models									
6.00	73	1.044	8.07	0.355	−0.320	1.648	−0.608	0.014	1.743
4.50	50	0.924	8.01	0.320	0.298	2.023	0.001	0.648	4.377
4.00	46	0.900	7.99	0.304	0.404	2.133	0.193	0.948	5.729
3.50	36	0.883	7.97	0.270	0.360	2.216	0.373	1.184	6.997
3.00	39	0.841	7.93	0.261	0.677	2.457	0.696	1.837	12.570
2.50	52	0.806	7.89	0.270	0.739	2.677	0.983	2.436	21.029
2.00	50	0.784	7.82	0.271	1.268	2.652	1.033	1.940	22.075
1.50	28	0.731	7.03	0.260	2.033	0.156	0.948	0.385	16.285
S06C models									
5.00	54	0.956	8.03	0.334	0.018	1.856	−0.250	0.377	2.907
4.50	47	0.921	8.01	0.317	0.083	1.973	−0.059	0.585	3.825
4.00	40	0.890	7.98	0.295	0.389	2.109	0.283	0.997	5.580
3.50	21	0.846	7.95	0.270	0.251	2.202	0.490	1.310	6.998
3.00	31	0.830	7.92	0.251	0.675	2.270	0.747	1.518	9.168
2.50	23	0.758	7.51	0.253	1.833	0.510	1.113	0.428	12.840
2.00	21	0.702	7.03	0.260	1.534	0.476	0.621	0.338	5.714
1.70	18	0.685	6.88	0.253	1.573	0.053	0.578	0.059	5.909
1.50	15	0.675	6.76	0.253	1.388	0.107	0.469	0.082	4.040
1.20	14	0.660	6.57	0.253	1.141	0.056	0.412	0.056	2.608
1.00	13	0.671	6.37	0.259	2.131	0.073	1.311	0.144	23.516

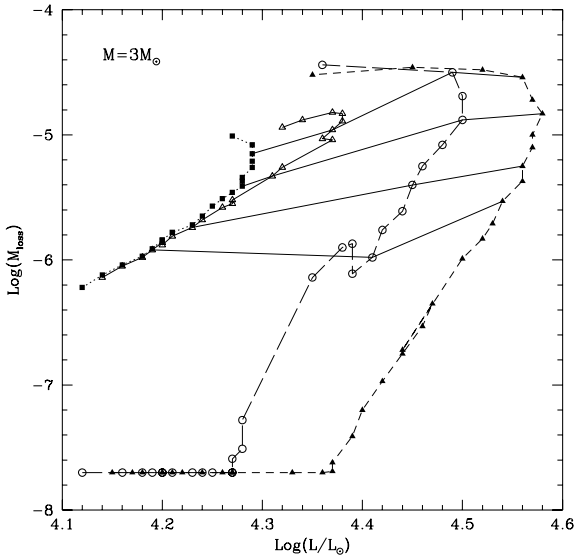

Figure 1. Evolution of the mass-loss rate ($\dot{M}$ in $M_\odot\,yr^{-1}$) as a function of the surface luminosity for models with initial masses of 3 $M_\odot$ calculated with different prescriptions for the mass-loss and molecular opacity (see Table 1 for the meaning of the various symbols). Each point in the plot marks the quiescent stage of the luminosity maximum, preceding the occurrence of a TP. The solid lines connect the four evolutionary sequences at the stage when the total mass of the star has been reduced to 2.9, 2.7, 2.5 and 2.0 $M_\odot$.

various symbols. Core H- and He-burning phases are not included in this plot, which starts from the beginning of the TP-AGB phase. Each point marks the quiescent stage of the pre-TP luminosity maximum. The solid lines are iso-mass locii and connect the four evolutionary sequences at the stages when the total mass of the star has been reduced to 2.9, 2.7, 2.5 and 2 $M_\odot$.

In all the four cases considered here, the 3-$M_\odot$ models share a few common features, namely: (i) they experience the HBB, which is usually associated with an overluminosity[4] effect, and (ii) they enter the domain of C stars, as the surface C/O ratio increases above unity due to the TDU. At the same time, significant differences arise.

The S06H and S06C models experience a much weaker mass-loss at the beginning, evolving at an approximately constant mass for many TPs; this is at odds with the behaviour of the BH and BC models, where an efficient mass-loss determines an earlier extinction of the HBB and its overluminosity (following a rapid cooling of the envelope structure). This circumstance is seen in the maximum luminosity attained, which is ∼0.2 dex fainter than in S06H and S06C sequences.

The role played by the opacity treatment can be understood by examining the evolution of models sharing the same description of mass-loss, for example, the S06H and S06C models. In the latter, the rapid increase in the mass-loss rate as soon as the surface C/O exceeds unity (clearly detectable as a jump in $\dot{M}$) favours an earlier reduction in the mass of the external mantle, which again causes an earlier drop in the luminosity L (we have a ∼0.1 dex difference in the maximum luminosity in this case). The drop in L is associated with a lower temperature at the bottom of the convective envelope, that is, less-favourable conditions for the HBB. We may conclude that, in general, using a mass-loss description is only mildly dependent on the luminosity and/or neglecting the changes in the molecular chemistry in the opacity computations, when C/O > 1, corresponds to larger temperatures in the external mantle, in favour of a more efficient HBB.

[4] In quiescent stages, TP-AGB models with the HBB are brighter than expected by the classical core mass–luminosity relation (e.g. Boothroyd & Sackmann 1992).

4.3 C-star stage and HBB quenching

Fig. 2 shows the evolution of the C–O core mass during the TP-AGB phase of models with different initial masses and/or input proscriptions. The BH and BC models (full squares and open triangles) evolve to smaller core masses as a result of the higher mass-loss in their early TP-AGB phase.

In the left-hand panel, we see that in the less-massive BH and BC models, the mass of the remnant is almost independent of the adopted opacity, being only slightly higher, as expected, in the BH case. When the S06 mass-loss rate is used (S06H and S06C models), the masses of the remnants differ more significantly (see column 3 of Table 2), the discrepancy consisting in $\delta M_C \sim 0.08\,M_\odot$ for $M = 2\,M_\odot$, $\delta M_C \sim 0.04\,M_\odot$ for $M = 2.5\,M_\odot$ and $\delta M_C \sim 0.02\,M_\odot$ for $M = 3.5\,M_\odot$. The difference in M_C is higher at lower masses, because these models reach more easily the C-rich stage, which is accompanied by an increase in the molecular opacity in the S06C models. The stronger sensitivity of the S06H and S06C models to the opacity treatment compared to the BH and BC models can be explained by the fact that the Blöcker (1995) formalism predicts quite high mass-loss rates, so that the models become C-rich when most of their envelope masses have already been lost, with a resulting little possibility of establishing great differences in the masses of the remnants.

The evolution of M_C for higher mass models is shown in the right-hand panel of Fig. 2. The BH and BC lines are again almost overimposed in this diagram and the differences between the S06H and S06C sets of models persist up to masses of the order of 4 $M_\odot$, whereas in more massive models, the surface C/O ratio hardly approaches unity, thus rendering the results almost opacity-independent. For the 4.5-$M_\odot$ model, we note that the tracks are practically split into two branches, according to the mass-loss treatment.

The description given above can be complemented with the behaviour of the temperature at the bottom of the convective envelope, T_{bce}. This is a key quantity to understand the degree of nucleosynthesis expected and thus the chemical composition of the ejecta. The evolution of T_{bce} as a function of the current stellar mass is shown for all models in Fig. 3.

For $M \leq 2.5\,M_\odot$, HBB conditions, that is, $T_{bce} \gtrsim 60 \times 10^6$ K, are never reached, with the only exception of the S06H models, where the relatively mild mass-loss, due both to the S06 prescription itself and to the molecular opacities that neglect CNO variations, favours the increase in the core mass and temperature at the bottom of the envelope, eventually reaching HBB conditions.

This is confirmed by the two panels of Fig. 4, showing the evolution of the surface carbon abundance for the two models with the initial masses 2.0 $M_\odot$ (left-hand panel) and 2.5 $M_\odot$ (right-hand panel). In the models BH (solid line) and BC (dotted line), the surface carbon increases with a step-like profile that is typical of TDU effects. The BC models undergo a smaller number of TPs as a consequence of the higher mass-loss rates experienced as the C/O ratio exceeds unity; their final carbon content is therefore lower.

An increasing trend of the carbon abundance is also shown by the S06C models (long-dashed lines), although in this case most of the carbon enhancement is achieved at the beginning, when the mass

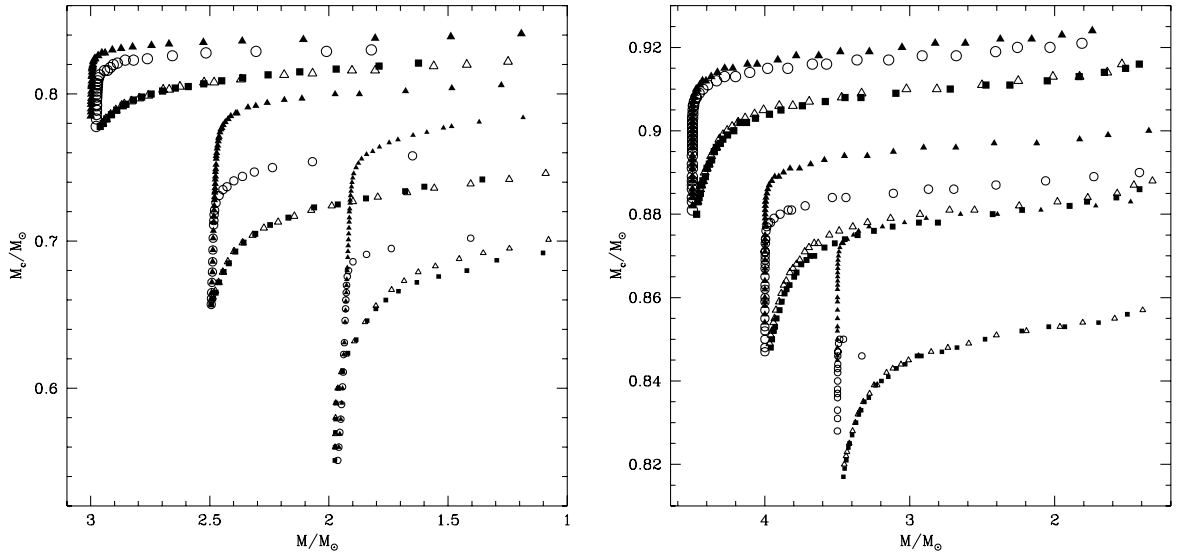

Figure 2. Left-hand panel: evolution of the core mass as a function of the current stellar mass for models with initial masses 2, 2.5 and 3 $M_{\odot}$. Each point on the tracks corresponds to the quiescent CNO burning phase before the occurrence of each TP. Refer to Table 1 for the meaning of the symbols. Right-hand panel: the same as the left-hand panel, but referring to the evolution of 3.5-, 4.0- and 4.5-$M_{\odot}$ models.

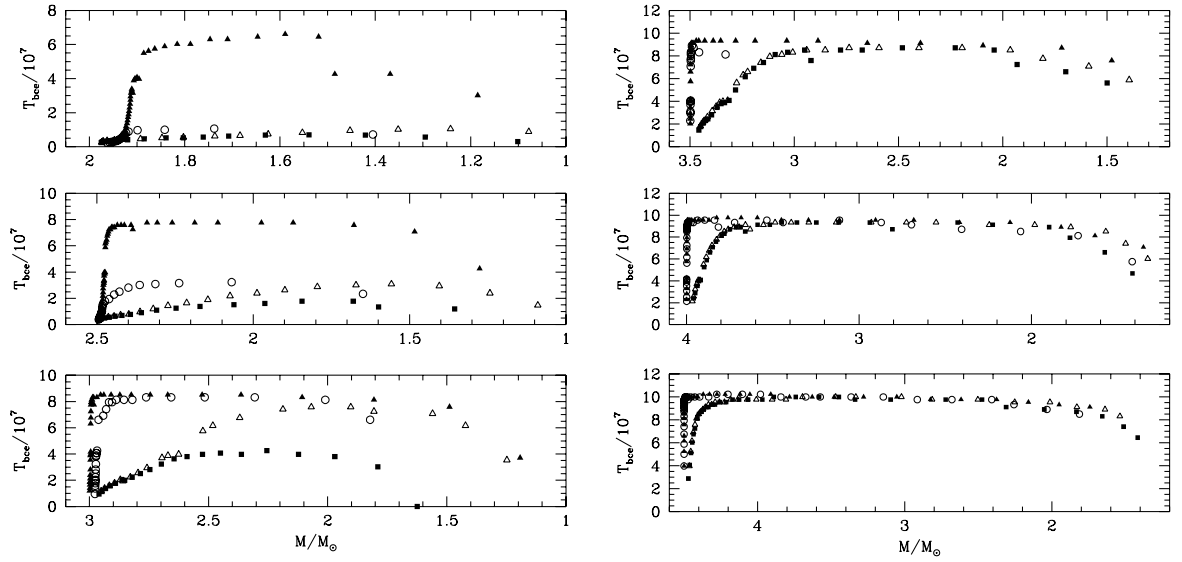

Figure 3. The same as Fig. 2, but showing the temperature at the bottom of the convective envelope

lost is negligible; at later stages, the strong mass-loss triggered by the formation of C-bearing molecules prevents further meaningful changes in the surface carbon mass fraction.

Different is the behaviour of the S06H models (dashed lines) in both the panels of Fig. 4: the fact that the HBB is operating can be recognized from the rapid drop in the surface carbon abundance (being converted into nitrogen). In these cases, the ejecta of the stars are expected to be carbon depleted.

Moving to higher masses, we see from Fig. 5 that in the 3-$M_{\odot}$ model, HBB conditions are reached in both the S06C and S06H models, whereas in the models calculated with the Blöcker (1995) mass-loss, the HBB is quenched when the correct opacities are adopted (compare the dotted and solid tracks in Fig. 5 and the corresponding evolution of $T_{\rm bce}$ marked by the open triangles and full squares in the bottom left-hand panel of Fig. 3). The HBB is found in all models of higher mass, as can be seen in the right-hand panels of Fig. 3. The only difference we see here is the different mass left in the envelope when the asymptotic temperature at the bottom of the envelope is reached. For the same reasons previously discussed, the S06H and S06C models reach this stage when only a small amount of mass has been lost: this will have some effects on the yields (see Section 5).

4.4 Summary

The results confirm the analysis by Marigo (2002) and the main findings of the investigation by Cristallo et al. (2008): low-mass AGB models need to be calculated with the correct low-T opacities that account for the changes in the molecular chemistry driven by variations in the C/O ratio and more generally in the CNO abundances. Neglecting the surface-carbon enrichment in the opacity computations delays the ejection of the external mantle, leads to a

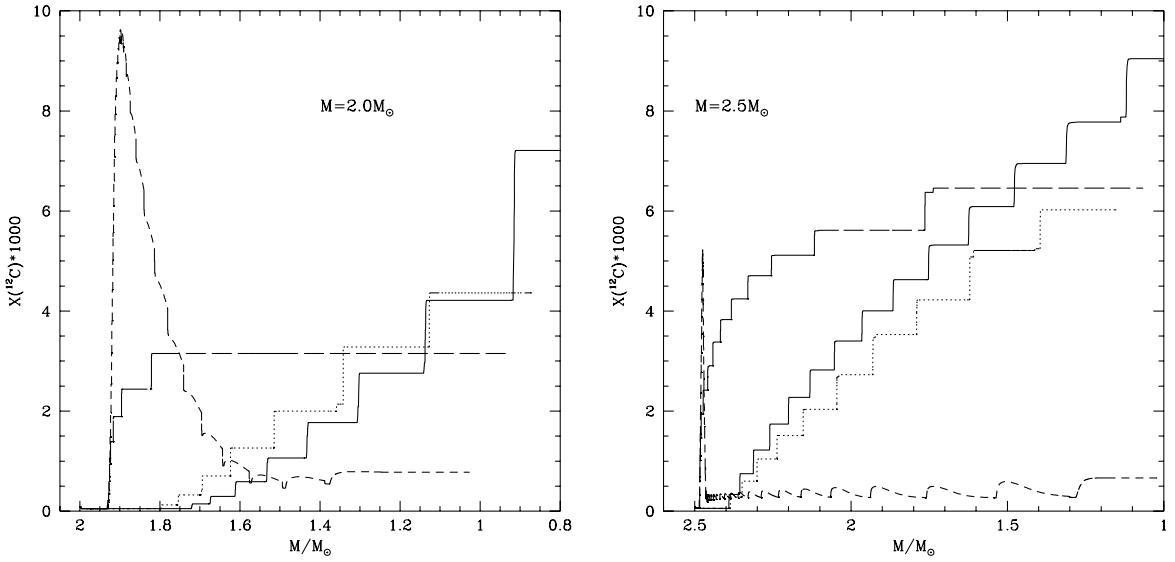

Figure 4. Left-hand panel: the variation in the surface carbon abundance in models with an initial mass $2\,M_{\odot}$, calculated for various treatments of the mass-loss and molecular opacities. Right-hand panel: the same as in the left-hand panel, but for models with $M = 2.5\,M_{\odot}$. The meaning of the different tracks is as follows: solid: BH models; dotted: BC; dashed: S06H; long-dashed: S06C.

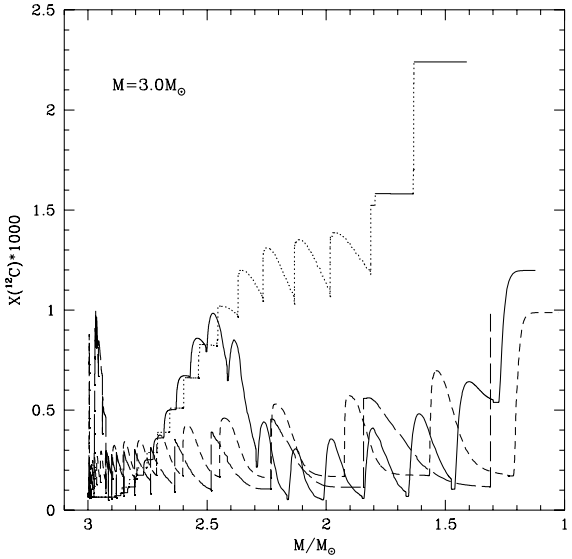

Figure 5. The same as Fig. 4, but referring to models with an initial mass of $3\,M_{\odot}$.

higher final core mass and, in more massive models, leads to higher temperatures at the envelope base, hence favouring the development of the HBB.

The extent of the changes introduced by a correct opacity computation is conditioned to the treatment of the mass-loss. The indirect effects of using C-rich opacities on the growth of the remnant core, maximum luminosity and temperature at the bottom of the convective envelope are larger when the mass-loss in the early AGB phase is sufficiently mild. In fact, under these circumstances, the C-rich stage is reached when the envelope still contains a large fraction of the mass; this applies, for instance, when a treatment like S06 is used. Models calculated with the Blöcker (1995) formula are less sensitive to the opacity changes.

The analysis on the HBB made by Marigo (2007) is confirmed. For the reasons mentioned above, the quenching of the HBB in models calculated with the Blöcker (1995) mass-loss description is restricted to a narrow range of masses (clustering around $3\,M_{\odot}$ in the present investigation). Conversely, when a more moderate mass-loss, for example, VW93 or the modification suggested by S06, is used, the extinction of the HBB involves a wider range of masses, which, in this investigation, spans the interval from 1.8 to $2.6\,M_{\odot}$.

All models with $M \geq 3.5\,M_{\odot}$ achieve HBB conditions, regardless of the opacity treatment, because the C/O ratio keeps in any case well below unity. Some differences between models differing in the mass-loss treatment persist up to $\sim$4.5 $M_{\odot}$ and tend to disappear for larger masses. As extensively discussed in Ventura & D'Antona (2005), in this range of masses, the key quantity that controls the activation and the strength of the HBB is the treatment of the convective instability and, specifically, the efficiency of convection.

5 HOW ROBUST ARE THE ASYMPTOTIC GIANT BRANCH YIELDS?

Changes in the surface chemical composition of AGB stars are caused by the HBB and TDU. The former keeps the overall C+N+O abundance constant,[5] whereas the TDU increases the carbon abundance, hence, the total C+N+O, independently of the possible later conversion (via HBB) of ^{12}C to ^{14}N at the bottom of the convective zone.

5.1 The C+N+O increase

In the context of the distinctive chemical patterns exhibited by GC stars, the surface C+N+O is a key quantity in the debate concerning the self-enrichment scenario by massive AGB stars (Ventura et al. 2001; D'Ercole et al. 2008), because the spectroscopic surveys of GC stars confirmed that the total C+N+O is approximately

[5] We recall that the invariance applies to the total C+N+O abundance expressed as a number fraction and not as a mass fraction: in fact, the CNO cycle preserves the total number of the CNO catalysts, not their total mass.

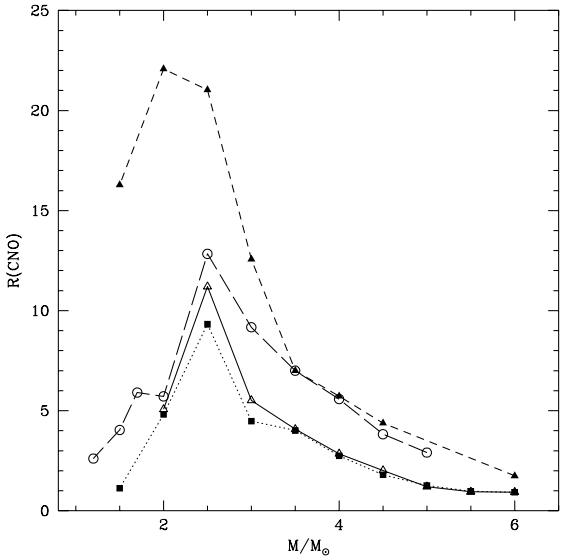

Figure 6. The CNO variation in the ejecta for the four sets of models under consideration. The ordinate shows R(CNO), that is, the ratio between the average C+N+O in the ejecta and the initial C+N+O content of the star. The meaning of the different lines is the same as given in Fig. 4.

constant (Ivans et al. 1999), even when comparing stars with different surface abundances of other elemental species. Therefore, AGB ejecta with a great CNO enhancement would rule out their role as the possible cause of the observed patterns (Karakas et al. 2006).

The CNO increase in the ejecta is shown in Fig. 6; this is the same quantity reported in column 10 of Table 2. In all cases, R(CNO) shows a maximum for $M \sim 2$–$2.5\,M_{\odot}$: lower masses experience fewer TDUs, whereas in more massive models, the effects of the TDU are reduced, due to dilution of the dredged-up, C-rich material into a massive envelope.

For $M \gtrsim 3.5\,M_{\odot}$, similarly to other quantities discussed in Section 4, R(CNO) depends mainly on the mass-loss prescription; the models split into two branches. S06H and S06C ejecta show a greater enhancement in the total CNO, due to the larger number of TPs and TDUs experienced. Interestingly, for $M \sim 6\,M_{\odot}$, the two branches tend to converge to unity (i.e. invariance of the total C+N+O), since these models are characterized by a quite efficient HBB and large luminosities, which lead to a quick ejection of the envelope.

For $M < 3.5\,M_{\odot}$, the treatment of the molecular opacities becomes more important: the CNO enhancement is lower for S06C and BC models compared to S06H and BH models. The largest R(CNO) is reached by the S06H models (dashed line) due to the great number of TPs experienced, while the others (BH, BC and VW models) show more similar trends.

The left-hand panel of Fig. 7 shows the chemical content of the ejecta on the [C/Fe] versus [N/Fe] plane. Models with the same mass are connected with continuous lines. The points in the lower right-hand corner correspond to low-mass models ($M \leq 2.5\,M_{\odot}$) not experiencing any HBB and are characterized by a large [C/Fe] as a consequence of the TDU. In general, a large value of [N/Fe] is a signature of the HBB. The spread in [N/Fe] relative to models with masses in the range 2–3 $M_{\odot}$ is a mere consequence of different (if any) degrees of the HBB achieved in these masses. S06H models (full triangles) constitute a sort of an upper envelope for the N enrichment: as discussed previously, these models experience a large number of TDUs and the HBB is always efficient.

Note the position of the 1.5-$M_{\odot}$, BC model, indicated by the full square with the lowest [N/Fe]: the chemical content of the mass ejected shows only a modest increase in carbon and no change in nitrogen, because the higher mass-loss quickly leads to an end of the AGB phase. This is also confirmed in Fig. 7 (right-hand panel) by the position of the same point in the [O/Fe]–[Na/Fe] plane, corresponding to [O/Fe] = +0.4 and [Na/Fe] = 0, that is, the initial chemical composition assumed for these stars.

Higher mass models experience a more powerful HBB, thus exhibiting a lower [C/Fe] in their ejecta. The TDU is less efficient in increasing the surface abundance of carbon when the dredged-up material is diluted into a massive envelope; this, in turn, favours a smaller production of nitrogen by p-captures by carbon nuclei.

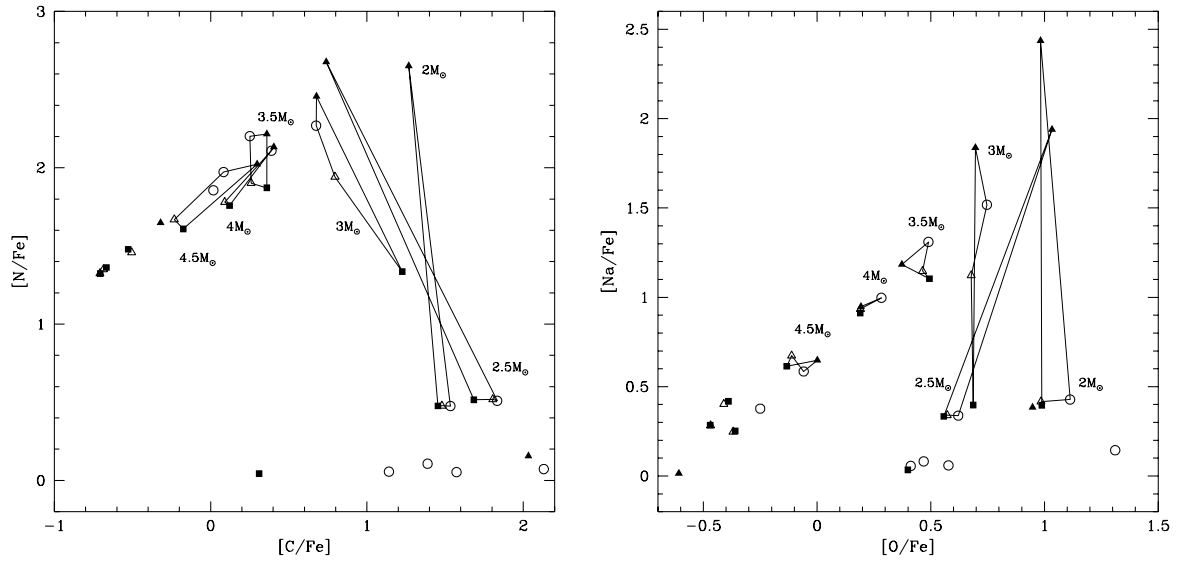

Figure 7. Carbon and nitrogen (left-hand panel) and oxygen and sodium (right-hand panel) contents in the AGB ejecta. Lines connect models with the same initial mass.

5.2 Sodium

The right-hand panel of Fig. 7 shows the oxygen and sodium content of the yields, in terms of [Na/Fe] versus [O/Fe]. These two elements are the main targets in the spectroscopic surveys of GCs and the oxygen–sodium anticorrelation is a well-established pattern observed in practically all the GCs (Carretta 2006).

The ejecta of the lowest masses are O-enriched (we recall that the initial abundance of our α-enhanced mixture is [O/Fe] = +0.4), due to the TDU. The S06C models (open circles) show a slightly higher [O/Fe], because they experience many TDUs, and the HBB is far from being activated, thus keeping the surface oxygen high. The greater is the mass, the lower is the oxygen content of the ejecta, due to the HBB, which destroys ^{16}O via p-captures in favour of ^{14}N.

The behaviour of sodium at the surface of AGB stars is described in details in Ventura & D'Antona (2008) (see their fig. 4). The surface sodium content is unchanged in the lowest masses (see also column 8 in Table 2), while increases in models ($M \geq 2\,M_{\odot}$), where the temperature at the bottom of the envelope is high enough to convert the dredged-up ^{22}Ne to Na. Similarly to nitrogen, the largest differences in [Na/Fe] due to the mass-loss and opacity prescriptions are found in those models with a mild HBB (note again the higher values attained by the S06H models). For higher temperatures, the destruction channel of Na via p-capture prevails over production, leading to the lower [Na/Fe] for larger stellar masses.

5.3 An overview on the uncertainties in the yields by AGB stars

The analysis developed so far allows us to have a first appraisal of the uncertainties affecting the yields from AGB stars produced by two main factors: mass-loss and low-T radiative opacities. We have explored two treatments of the mass-loss, which, especially in the early phases of the AGB evolution, differ considerably: in this way, our investigation should sample the present status of indetermination in the chemical yields.

In agreement with previous investigations, we confirm that using opacities coupled with the actual surface composition is mandatory for masses below a threshold value, corresponding to the full activation of the HBB, which in this work corresponds to $M \sim 3.5\,M_{\odot}$. When the changes in the molecular chemistry are correctly accounted for in the opacities, the attainment of the C-rich stage (C/O > 1) is usually accompanied by a sudden increase in the mass-loss, which favours the ejection of the whole mantle, speeding up the end of the AGB evolution. The enrichment in carbon and CNO is consequently lower.

Typically, the changes in the yields, determined by the use of correct opacities, are more significant in models, where a milder dependency of the mass-loss on the luminosity is adopted. In fact, this would correspond to a longer TP-AGB lifetime, during which the surface composition may be affected by (i) a larger number of TDU episodes, and (ii) more favourable conditions for the development of the HBB. Conversely, assuming a very efficient mass-loss formalism, as predicted by a Blöcker (1995)-like law, the accuracy loss introduced by unsuitable opacities (e.g. valid for scaled solar mixture) is less dramatic, since the C-rich stage is reached when a considerable fraction of the mass of the envelope is already lost.

Within this general trend, the sensitiveness of the yields to the model assumptions varies according to the mass of the star, as outlined below.

The largest uncertainties in the yields belong to stars for which the temperature at the bottom of the convective envelope is just sufficient to ignite the HBB, that is, 1.8–3.0 $M_{\odot}$. In particular, [N/Fe] and [Na/Fe] may vary by ∼2 dex, depending on the assumed input prescriptions. The oxygen yield is more robust.

At lower masses, that is, $M \sim 1.5\,M_{\odot}$, the results are more affected by the mass-loss description: the TDU does not even take place when the Blöcker (1995) prescription is followed, being prevented by a rapid expulsion of the external envelope.

Above 3.5 $M_{\odot}$, the opacity treatment become less influential and most of the uncertainty in the yields should be ascribed to the the mass-loss treatment.

This investigation has also shown that, although the yields may vary according to the adopted mass-loss rate in any range of mass, the predicted trends between different elemental species do not depend on the model assumptions, for example, the slopes in both the [C/Fe]–[N/Fe] and [O/Fe]–[Na/Fe] diagrams are preserved (see Fig. 7).

6 A COMPARISON WITH PREVIOUS INVESTIGATIONS

In view of testing the reliability of AGB models, we compare our results with investigations by other research groups, focusing on the the recent investigations by Weiss & Ferguson (2009) and Cristallo et al. (2009), in which low-T opacities are suitably calculated by considering the increase in the surface carbon abundance, an essential requirement to correctly describe C-rich stage.

We consider, in particular, the models computed with the same initial mass, 2.0 $M_{\odot}$, that include our S06C and BC models, the $Z = 0.001$ model by Cristallo et al. (2009) (see their table 3) and the $Z = 5 \times 10^{-4}$ model by Weiss & Ferguson (2009) (see their table B.4). Although the initial chemical compositions are not the same [Cristallo et al. (2009) used a scaled solar mixture with $Z = 0.001$, whereas Weiss & Ferguson (2009) adopted an α-enhanced mixture with $Z = 0.0005$], the main differences can be explained in terms of the different input prescriptions.

One striking feature is the different number of TPs experienced, that is, 19 in Cristallo et al. (2009), 21 and 16 in the two S06C and BC cases, respectively, and only six in Weiss & Ferguson (2009), despite the fact that the latter model corresponds to the lowest metallicity. The small number of TPs found in Weiss & Ferguson (2009) is accompanied by a shorter AGB lifetime, which is approximately one-third of our estimated values. Due to the absence of the HBB, we rule out convection as a possible cause of such a discrepancy and focus on the other two, uncertain, physical inputs, that is, mass-loss and the treatment of the convective borders, particularly during the TDU phase.

Let us first focus on the effect produced by different mass-loss treatments. Fig. 8 shows the evolution of the mass-loss rate in our 2.0-$M_{\odot}$ AGB model computed with the ATON code, assuming CNO-variable molecular opacities and three choices for $\dot{M}$, namely S06 (open circles), Blöcker (1995) (open triangles) and Weiss & Ferguson (2009) (full squares). We recall that the latter scheme assumes a Reimers' formula up to a threshold pulsational period of 400 d, followed by the Wachter et al. (2008) rate when the C-star stage is reached.

We note that the S06 treatment favours rates significantly smaller, particularly at the beginning of the AGB phase, with differences up to ∼1.5 dex compared to the others. A smaller difference exists between the Blöcker (1995) and the Weiss & Ferguson (2009)

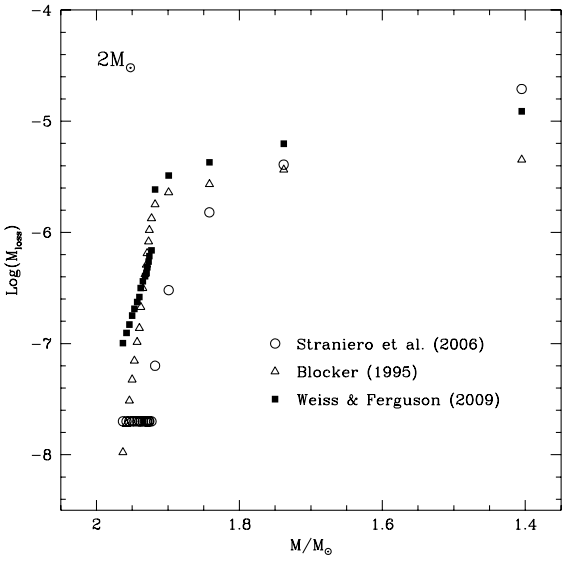

Figure 8. Mass-loss rates experienced by a 2-$M_\odot$ model, computed with the ATON code, according to various mass-loss prescriptions available in the literature.

recipes, the latter being higher by ∼0.2–0.3 dex during most of the evolution.

In the early AGB phase, the Weiss & Ferguson (2009) treatment predicts rates of the order of 10^{-7}–10^{-6} $M_\odot$ yr^{-1}, which are, however, not sufficient to diminish the total number of TPs to 6, which is their original result. This suggests that the main reason for the smaller number of TPs in the Weiss & Ferguson (2009) investigation compared to our models is an earlier transition to the C-star stage. This difference is due to two reasons: (i) the modelling of the convective overshoot from the bottom of the envelope (see their equation 2), based on an exponential decay of the diffusive coefficient, with the same e-folding distance used for main-sequence width fitting. This approach determines a much deeper extension of the TDU when compared with our models (where no overshoot is assumed) and with those by Cristallo et al. (2009), who adopted an exponential decay of the convective velocity from the inner border of the external mantle, with an e-folding distance tuned in order to allow the synthesis of a given amount of ^{13}C available for n-captures. This extramixing used by Cristallo et al. (2009) explains their smaller number of TPs, when compared to our S06C model, and the different final core masses (0.67 $M_\odot$, to be compared to 0.70 $M_\odot$); and (ii) the convective overshoot from the He-burning shell adopted by Weiss & Ferguson (2009) and neglected here and in Cristallo et al. (2009), which, as described by Herwig & Austin (2004), renders the pulses stronger. The models presented here, though including no overshoot, are much more similar to those presented by Cristallo et al. (2009), in terms of the duration of the whole AGB phase and the chemistry of the ejecta.

A detailed investigation of the TDU phenomenology and the possible effects of assuming some convective overshoot from the bottom of the convective envelope is beyond the scope of this paper; interested readers may find in Herwig (2000), Herwig (2005), Mowlavi (1999) and Straniero et al. (1997) a full discussion on the key issues relevant to address this problem.

Anyhow, this study clearly illustrates that the AGB evolution is the product of a complex interplay between various processes: the treatment of the extramixing, for instance, has a remarkable impact not only on the chemical but also on the physical properties of these stars.

7 CONCLUSIONS

To test the robustness of the results provided by AGB modelling (or at least to quantify the uncertainty range), we have investigated the sensitivity of the main physical and chemical properties to the choices inherent the input macro- and micro-physics.

We find a threshold mass, that is, $M \simeq 3.5\,M_\odot$, for $Z = 0.001$ in the present analysis (note that it also depends on the assumed overshooting from the central regions during the core H- and He-burning), above which the results are little sensitive to the opacity treatment, because the HBB prevents the surface C/O ratio to exceed unity.

In this range of masses, a mass-loss modelling plays a crucial role. Models calculated with a treatment of the mass-loss, only mildly dependent on the luminosity, such as the classic VW93 or the S06 recipe used here, predict smaller rates during most of the AGB phase; thus, more TPs are experienced. This also favours the growth of the luminosity and temperature at the bottom of the convective zone and a more advanced HBB nucleosynthesis: the yields will contain the signature of a p-capture nucleosynthesis, for example, lower carbon and oxygen abundances, and higher nitrogen content. However, the general patterns of the C–N and O–Na relations and the very small increase in the overall CNO abundance are almost independent of the opacity and mass-loss treatment: we expect that a convection modelling plays a relevant role here, in agreement with the analysis by Ventura & D'Antona (2005).

For masses smaller than 3.5 $M_\odot$, the interplay between the opacity and mass-loss treatment is more tricky, because the lack of the HBB favours increase in surface carbon. Generally speaking, we confirm the results by Marigo (2002, 2007), Cristallo et al. (2008, 2009) and Weiss & Ferguson (2009): the use of the correct opacities in the low-T regime speeds up the loss of the stellar envelope via the strong winds associated with the general expansion of the structure, when the surface C/O ratio exceeds unity. We expect in this case a smaller number of TPs and a less-advanced nucleosynthesis (if any) at the bottom of the convective envelope.

Models calculated with a mass-loss rate steeply dependent on the luminosity show a more homogeneous behaviour, whereas when a milder dependency of $\dot{M}$ with the luminosity, for example, a relationship that relates $\dot{M}$ to the stellar period, is adopted, many physical properties, for example, the core mass, temperature at the bottom of the convective zone and total number of TPs experienced, follow a completely different behaviour. In this case, quenching of the HBB determined by the use of the C-rich opacities, predicted by Marigo (2007), is confirmed, being a common feature for all the models with masses in the range 1.8–3.0 $M_\odot$. A narrower range of masses (around ∼3 $M_\odot$) is otherwise affected by this uncertainty, when an efficient mass-loss prescription, like the Blöcker (1995) formula, is adopted.

Contrary to the models experiencing the HBB, the yields from lower mass stars are highly uncertain and model-dependent: the average [C/Fe] in the ejecta shows up an overall uncertainty of 0.7 dex, though this difference reduces to ∼0.3–0.4 dex, if models calculated with the same opacities are compared. The situation for nitrogen and sodium is more extreme, as they are particularly sensitive to the ignition of the HBB. The differences in [N/Fe] and [Na/Fe] can reach ∼2 dex, and even when comparing models with the same assumptions for the opacity treatment, discrepancies of an

order of magnitude still persist. The oxygen yields appear, instead, more stable.

These trends should be considered representatives of AGB models with a low metal content ($Z \sim 0.001$), while they need to be further explored at larger metallicities, typical of stars in the Large Magellanic Cloud (Ventura et al., in preparation). Moreover, in the present unresolved scenario about the efficiency of the TDU and mass-loss, a valuable contribution may come from synthetic AGB models, that is, via a thorough calibration of AGB properties as a function of the stellar mass and metallicity based on a large set of observables (Hertzsprung–Russell diagrams including the mid-infrared, C/M star ratios, chemistry of atmospheres and planetary nebulae, initial–final mass relation, integrated colours and brightness fluctuations). This work is in progress.

ACKNOWLEDGMENT

PM acknowledges financial support by the University of Padova (60A02-2949/09), INAF/PRIN07 (CRA 1.06.10.03) and MIUR/PRIN07 (prot. 20075TP5K9).

REFERENCES

Abia C., Boffin H. M. J., Isern J., Rebolo R., 1991, A&A, 245, L1
Angulo C. et al., 1999, Nucl. Phys. A, 656, 3
Battinelli P., Demers S., 2004, A&A, 418, 33
Bedijn P. J., 1988, A&A, 205, 105
Blanco V. M., Blanco B. M., McCarthy M. F., 1980, ApJ, 242, 938
Blöcker T., 1995, A&A, 297, 727
Blöcker T., Schöenberner D., 1991, A&A, 244, L43
Blum R. D. et al., 2006, AJ, 132, 2034
Bolatto A. D. et al., 2007, ApJ, 655, 212
Boothroyd A. I., Sackmann I.-J., 1992, ApJ, 393, L21
Bowen G. H., 1988, ApJ, 329, 299
Bowen G. H., Willson L. A., 1991, ApJ, 375, L53
Bressan A., Chiosi C., Fagotto F., 1994, ApJS, 94, 63
Bruzual G., Charlot S., 2003, MNRAS, 344, 1000
Burbidge E. M., Burbidge G. R., Fowler W. A., Hoyle F. B, 1957, Rev. Modern Phys., 29, 547
Busso M., Gallino R., Wasserburg G. J., 1999, ARA&A, 37, 239
Canuto V. M. C., Mazzitelli I., 1991, ApJ, 370, 295
Carretta E., 2006, AJ, 131, 1766
Cioni M. R., Habing H. J., Loup C., Groenewegen M. A. T., Epchtein N., Consortium T. D., 1999, in Whitelock P., Cannon R., eds, Proc. IAU Symp. 192, The Stellar Content of Local Group Galaxies. Astron. Soc. Pac., San Francisco, p. 65
Cloutman L. D., Eoll J. G., 1976, ApJ, 206, 548
Cristallo S., Straniero O., Lederer M. T., Aringer B., 2008, ApJ, 667, 489
Cristallo S., Straniero O., Gallino R., Piersanti L., Dominguez I., Lederer M. T., 2009, ApJ, 696, 797
D'Ercole A., Vesperini E., D'Antona F., Mc Millan S. L. W., Recchi S., 2008, MNRAS, 391, 825
Denissenkov P., Herwig F., 2003, ApJ, 590, L99
Fenner Y., Campbell S., Karakas A. I., Lattanzio J. C., Gibson B. K., 2004, MNRAS, 353, 789
Formicola A. et al., 2004, Phys. Lett. B, 591, 61
Frogel J. A., Mould J., Blanco V. M., 1990, ApJ, 352, 96
Fujimoto M. Y., Nomoto K., Sugimoto D., 1976, PASJ, 28, 89
Grevesse N., Sauval A. J., 1998, Space Sci. Rev., 85, 161
Groenewegen M. A. T., de Jong T., 1993, A&A, 267, 410
Groenewegen M. A. T., Sloan G. C., Soszyński I., Petersen E. A., 2009, A&A, 506, 1277
Gullieuszik M., Rejkuba M., Cioni M. R., Habing H. J., Held E. V., 2007, A&A, 475, 467
Gullieuszik M., Held E. V., Rizzi L., Girardi L., Marigo P., Momany Y., 2008, MNRAS, 388, 1185
Hale S. E., Champagne A. E., Iliadis C., Hansper V. Y., Powell D. C., Blackmon J. C., 2002, Phys. Rev. C, 65, 5801
Hale S. E., Champagne A. E., Iliadis C., Hansper V. Y., Powell D. C., Blackmon J. C., 2004, Phys. Rev. C, 70, 5802
Held E. V., Gullieuszik M., Rizzi L., Girardi L., Marigo P., Saviane I., 2010, MNRAS, 404, 1475
Herwig F., 2000, A&A, 360, 952
Herwig F., 2005, ARA&A, 43, 435
Herwig F., Austin S. M., 2004, ApJ, 613, L73
Iben I. J., 1975, ApJ, 196, 525
Iben I. J., Renzini A., 1982, ApJ, 263, L23
Iglesias C. A., Rogers F. J., 1996, ApJ, 464, 943
Ita Y. et al., 2008, PASJ, 60, 435
Ivans I. I., Sneden C., Kraft R. P., Suntzeff N. B., Smith V. V., Langer G. E., Fulbright J. P., 1999, AJ, 118, 1273
Izzard R., Tout C. A., Karakas A. I., Pols O. R., 2004, MNRAS, 350, 407
Karakas A. I., Lattanzio J. C., 2007, PASA, 24, 103
Karakas A. I., Fenner Y., Sills A., Campbell S. W., Lattanzio J. C., 2006, Mem. Soc. Astron. Ital., 77, 858
Maraston C., 2005, MNRAS, 362, 799
Marigo P., 2002, A&A, 387, 507
Marigo P., 2007, A&A, 467, 1139
Marigo P., Aringer B., 2009, A&A, 508, 1539
Marigo P., Girardi L., 2007, A&A, 469, 239
Marigo P., Girardi L., Bressan A., 1999, A&A, 344, 123
Mazzitelli I., 1979, A&A, 79, 251
Menzies J., Feast M., Whitelock P., Olivier E., Matsunaga N., da Costa G., 2008, MNRAS, 385, 1045
Merrill P. W., 1952, Sci, 115, 484
Mowlavi N., 1999, A&A, 344, 617
Nikolaev S., Weinberg M. D., 2000, ApJ, 542, 804
Piotto G. et al., 2007, ApJ, 661, L53
Reimers D., 1975, psae.book, 229
Renzini A., Voli M., 1981, A&A, 94, 175
Sackmann I. J., Boothroyd A. I., 1992, ApJ, 392, L71
Santini P. et al., 2009, A&A, 504, 751
Saumon D., Chabrier G., Van Horn H. M., 1995, ApJS, 99, 713
Scalo J. M., Despain K. H., Ulrich R. K., 1975, ApJ, 196, 805
Schröder K.-P., Cuntz M., 2005, ApJ, 630, L73
Smith V. V., Lambert D. L., 1989, ApJ, 345, L75
Smith V. V., Lambert D. L., 1990, ApJ, 361, L69
Stoltzmann W., Blöcker T., 2000, A&A, 361, 1152
Straniero O., Gallino R., Cristallo S., 2006, Nucl. Phys. A, 777, 311 (S06)
Straniero O., Chieffi A., Limongi M., Busso M., Gallino R., Arlandini C., 1997, ApJ, 332, 339
van den Hoek L. B., Groenewegen M. A. T., 1997, A&AS, 123, 305
van Loon J., Cioni M. R., Zijlstra A., Loup C., 2005, A&A, 438, 273
Vassiliadis E., Wood P. R., 1993, ApJ, 413, 641 (VW93)
Ventura P., D'Antona F., 2005, A&A, 341, 279
Ventura P., D'Antona F., 2008, A&A, 479, 805
Ventura P., Marigo P., 2009, MNRAS, 399, L54
Ventura P., D'Antona F., Mazzitelli I., 2000, A&A, 363, 605
Ventura P., D'Antona F., Mazzitelli I., Gratton R., 2001, ApJ, 550, L65
Ventura P., Zeppieri A., Mazzitelli I., D'Antona F., 1998, A&A, 334, 953
Wachter A., Schröder K. P., Winters J., Arndt T., Sedlmayr E., 2002, A&A, 384, 452
Wachter A., Winters J. M., Schröder K.-P., Sedlmayr E., 2008, A&A, 486, 497
Weiss A., Ferguson J. W., 2009, A&A, 508, 1343
Whitelock P., Menzies J., Feast M., Matsunaga N., Tanabè T., Yoshifusa I., 2009, MNRAS, 394, 795

This paper has been typeset from a TEX/LATEX file prepared by the author.